Novel Phenomenological Discrete Bubble Model of Freely Bubbling Dense Gas–Solid Fluidized Beds: Application to Two-Dimensional Beds

Salman Movahedirad and Asghar Molaei Dehkordi
Dept. of Chemical and Petroleum Engineering, Sharif University of Technology, Tehran, Iran

Niels Gerbrand Deen, Martin van Sint Annaland, and J. A. M. (Hans) Kuipers
Dept. of Chemical Engineering and Chemistry, Eindhoven University of Technology, P.O. Box 513, 5600 MB Eindhoven, The Netherlands

DOI 10.1002/aic.13729
Published online January 17, 2012 in Wiley Online Library (wileyonlinelibrary.com).

A phenomenological discrete bubble model has been developed for freely bubbling dense gas–solid fluidized beds and validated for a pseudo-two-dimensional fluidized bed. In this model, bubbles are treated as distinct elements and their trajectories are tracked by integrating Newton's equation of motion. The effect of bubble–bubble interactions was taken into account via a modification of the bubble velocity. The emulsion phase velocity was obtained as a superposition of the motion induced by individual bubbles, taking into account bubble–bubble interaction. This novel model predicts the bubble size evolution and the pattern of emulsion phase circulation satisfactorily. Moreover, the effects of the superficial gas velocity, bubble–bubble interactions, initial bubble diameter, and the bed aspect ratio have been carefully investigated. The simulation results indicate that bubble–bubble interactions have profound influence on both the bubble and emulsion phase characteristics. Furthermore, this novel model may become a valuable tool in the design and optimization of fluidized-bed reactors. © 2012 American Institute of Chemical Engineers *AIChE J,* 58: 3306–3317, 2012
Keywords: gas–solid fluidized beds, bubble, emulsion, discrete bubble modeling, bubble interaction

Introduction

In dense gas–solid fluidized beds, there are regions with a low fraction of solid particles, referred to as ''voids'' or ''bubbles.'' The latter are different from the bubbles present in gas–liquid systems, because there is no surface tension in these bubbles and gases can flow through the boundaries of bubbles. A common approach in the modeling of gas–liquid contactors is the discrete bubble model (DBM) approach, which is in fact an Eulerian–Lagrangian model.[1,2] Recently, a number of investigators used this approach in the modeling of gas–solid fluidized beds.[3,4] In this approach, each bubble is regarded as a distinct element that is tracked by integration of Newton's equation of motion. In this model, the equations of the emulsion phase, that is, a mixture of solids and gas, are solved using computational fluid dynamics (CFD) techniques. Actually, a set of discretized Navier–Stokes equations is solved for discrete points in the flow domain. Usually, the solution of these equations is very time consuming because small grid cells need to be chosen to arrive at grid–independent results. Bokkers et al.[3] published a paper on the modeling of large-scale fluidized beds using the DBM. They used CFD techniques to determine the emulsion phase flow pattern. Later, the model was extended to account for the effects of bubble–bubble interactions.[4]

Pannala et al.[5,6] developed a dynamic interacting bubble simulation for ozone decomposition in a gas–solid fluidized bed. Actually, their model is a DBM but the main deficiency of their model is that it can not predict the solid circulation patterns in the bed. The final goal of developing DBM for gas–solid fluidized beds is to apply this model for large-scale industrial fluidized beds, therefore, it is tempting to find simpler models, which can predict the hydrodynamic behavior of fluidized beds without having to resort to time-consuming CFD techniques. Therefore, in this work, a phenomenological DBM (PDBM) has been developed. In this modeling approach, the individual bubbles are tracked by evaluating the net force acting on each bubble. For a single isolated bubble, these forces include the drag force of emulsion phase on the bubble as well as the gravity and buoyancy forces. Both the bubble and emulsion phase flow patterns are significantly affected by the bubble–bubble interactions. For example, Krishna and van Baten[7] reported that the bubble velocity in the presence of other bubbles in gas–solid fluidized beds increases by a factor of 1.5−3.0 relative to the velocity of a single isolated bubble. Laverman et al.[4] have studied this effect and showed that bubble movement is considerably influenced due to the effect of bubble–bubble interactions. The models of bubble–bubble interactions are well developed.[8,9] In typical forms of these models, the velocity

Correspondence concerning this article should be addressed to A. Molaei Dehkordi at amolaeid@sharif.edu.

Table 1. The Assumptions of the Model Presented by Clift and Grace[8]

Bubble and wake shape	Single doublet
Basis for pressure distribution	Particulate phase treated as ideal fluid
Pressure constant around points	The nose of two bubbles N_1 and N_2 (Figure 1)
Tailing bubble (i) velocity in vertical direction under the effect of leading bubble (j)*	$v_{y,i} = v_{b\infty,i} + l_{ij}v_{y,j} + m_{ij}v_{x,j}$
Tailing bubble (i) velocity in horizontal direction under the effect of leading bubble (j)*	$v_{x,i} = m_{ij}v_{y,j} + n_{ij}v_{x,j}$

*Definition of the coefficients given in the text.

of a bubble in swarm of bubbles can be estimated by introducing a modification term, that is, the sum of effects of its leading bubbles to the velocity of a single isolated bubble.

To evaluate the emulsion phase flow pattern around a single bubble, de Korte et al.[10] supposed that each point in the emulsion phase could be considered as a bubble with zero size. They used bubble–bubble interaction relationships to describe the induced emulsion phase motion near the bubble. In this work, almost the same approach was used to describe the emulsion phase velocity field.

Anticipated difficulties in the validation of these models for three-dimensional (3-D) fluidized beds persuaded the present authors to develop a 2-D model to validate the model predictions with reported data obtained by noninvasive optical techniques such as particle image velocimetry (PIV) and digital image analysis (DIA) in pseudo-2-D fluidized beds. However, the developed models will be extended to full 3-D fluidized beds in the future.

Model

Bubble dynamics

To model bubble dynamics, the Newton's equation of motion can be solved for each bubble. The general form is given by

$$m_b \frac{d\vec{v}}{dt} = \vec{F}_t \tag{1}$$

where m_b, $\vec{v}$, and $\vec{F}_t$ are the bubble mass, bubble velocity, and total force acting on the bubble, respectively. Moreover, the total force acting on a single bubble can be expressed as

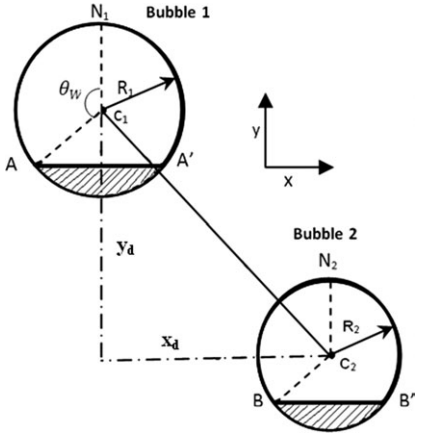

Figure 1. A pair of interacting bubbles.

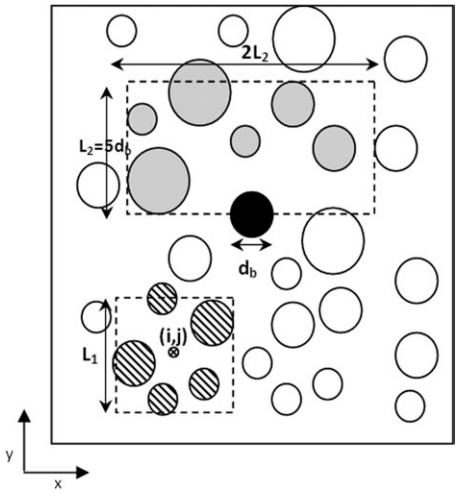

Figure 2. Neighbor lists for a bubble and an emulsion phase grid point (*i*,*j*).

$$\vec{F}_t = \vec{F}_G + \vec{F}_P + \vec{F}_D + \vec{F}_{vm} \tag{2}$$

where $\vec{F}_G$ is the gravity force, $\vec{F}_P$ is the pressure force, $\vec{F}_D$ is the drag force due to the presence of the emulsion phase, and $\vec{F}_{vm}$ is the virtual mass or added mass force, which is a force acting on the bubble via accelerating particles around it. The closures for the aforementioned forces acting on each bubble are summarized below.

Drag force

The general formula for calculating the drag force acting on a single 2-D bubble (disk shape) can be represented as

$$\vec{F}_D = -\frac{1}{2} C_D \rho_e \delta d_b |\vec{v} - \vec{u}|(\vec{v} - \vec{u}) \tag{3}$$

where C_D is the drag coefficient, ρ_e is the emulsion phase bulk density, δ is the bed depth, d_b is the bubble diameter, and $\vec{v}$ and $\vec{u}$, respectively, denote the bubble velocity and the local emulsion phase velocity. For pseudo 2-D beds, the drag coefficient is related to the correlations proposed for the bubble rise velocity. For 3-D beds, Davies and Taylor[11]

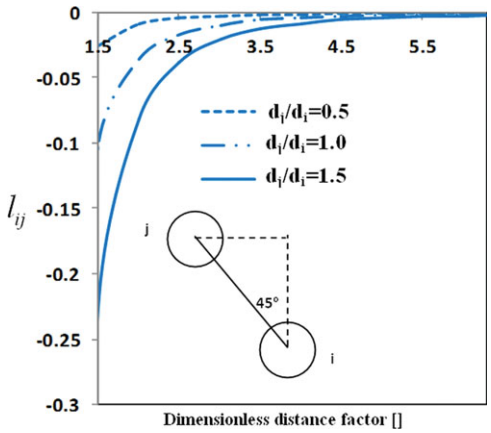

Figure 3. Variation of l_{ij} with dimensionless distance of two bubbles.

[Color figure can be viewed in the online issue, which is available at wileyonlinelibrary.com.]

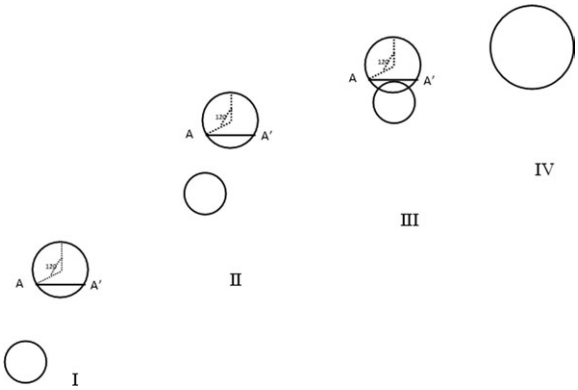

Figure 4. Delayed bubble coalescence scenario (θ_w = 120°).

proposed the well-known relationship for bubbles far enough from the side walls as follows:

$$v_{br} = c\sqrt{g d_b} \quad \text{with} \quad c = 0.711 \tag{4}$$

For 2-D beds, various relationships were reported in the literature.[12,13] Mudde et al.[12] proposed a constant coefficient of $c = 0.5$–0.6 for polymeric particles, whereas Shen et al.[13] proposed a coefficient between 0.8 and 1.0 for c in a bed filled with sand particles. The momentum balance for a single rising bubble at steady state yields

$$\vec{F}_G + \vec{F}_P + \vec{F}_D = 0 \tag{5}$$

or for a 2-D bed with a depth δ

$$-\frac{1}{2} C_D \rho_e d_b \delta v_{br}^2 + \rho_e g \pi \frac{{d_b}^2}{4} \delta - \rho_g g \pi \frac{{d_b}^2}{4} \delta = 0 \tag{6}$$

yielding

$$C_D v_{br}^2 = \left(\frac{\rho_e - \rho_g}{\rho_e}\right) \frac{\pi}{2} g \, d_b \tag{7}$$

$$C_D = \frac{\left(\frac{\rho_e - \rho_g}{\rho_e}\right) \frac{\pi}{2}}{c^2} \tag{8}$$

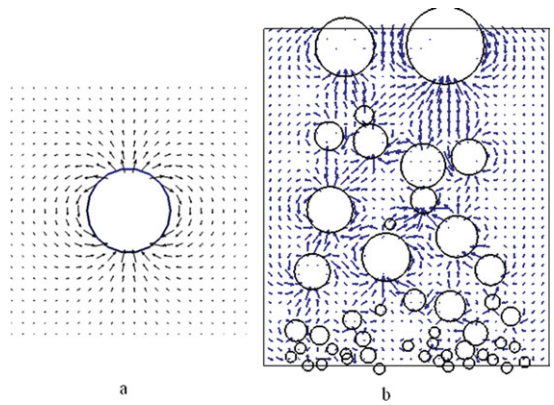

Figure 5. (a) Induced emulsion phase flow pattern due to the rise of a single isolated bubble and (b) a swarm of bubbles.

[Color figure can be viewed in the online issue, which is available at wileyonlinelibrary.com.]

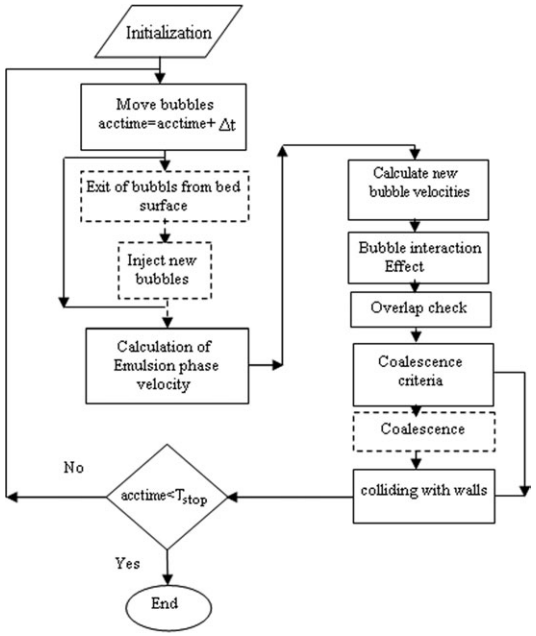

Figure 6. Flowchart of solution algorithm.

Assuming $\rho_e >> \rho_g$ and taking $c = 0.711$ leads to the following drag coefficient

$$C_D \approx \pi \tag{9}$$

Virtual mass force

As mentioned earlier, the virtual or added mass force is defined as the force acting on a bubble via accelerating particles around it. This force can be evaluated as follows[14]:

$$\vec{F}_{vm} = -C_{vm} \rho_e V_b \left(\frac{D\vec{v}}{Dt} - \frac{D\vec{u}}{Dt}\right) \tag{10}$$

where C_{vm} is the virtual mass coefficient equal to 0.5 for spheres and the derivatives are the substantial derivatives.

Bubble–bubble interactions

When a bubble is located at the rear of another bubble in a fluidized bed, its velocity changes due to the effect of its leading bubble. Clift and Grace[8,9] proposed a model for bubble–bubble interactions assuming each bubble and wake as a single doublet. They assumed that the velocity of a bubble in a fluidized bed might be approximated by adding to its rise velocity in isolation, the velocity that the particulate phase would have at the position of the nose if the bubble was absent. Other assumptions of their model are summarized in Table 1.

In a pair of bubble, the velocity of a tailing bubble (2) is affected by the leading bubble (1) as follows[9] (Figure 1):

$$v_{y,2} = v_{b\infty,2} + l_{21} v_{y,1} + m_{21} v_{x,1} \text{ in } y \text{ direction} \tag{11a}$$

$$v_{x,2} = m_{21} v_{y,1} + n_{21} v_{x,1} \text{ in } x \text{ direction} \tag{11b}$$

where $v_{b\infty}$ represents the rise velocity of an isolated bubble, v_x and v_y are bubble velocity components in the x and y

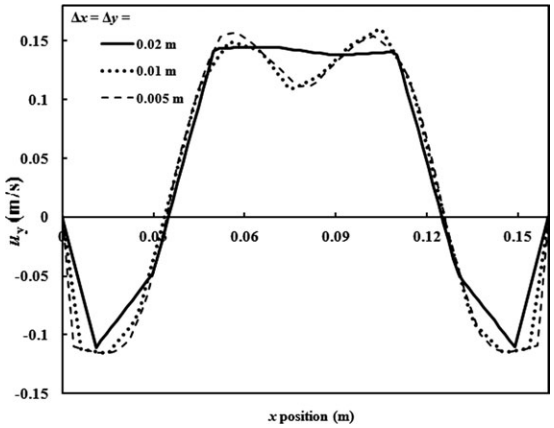

Figure 7. Dependency of predicted results on the mesh size.

directions, respectively, and l_{21}, m_{21}, and n_{21} can be given by

$$l_{21} = \frac{\left|(y_2 - y_1 + R_2)^2 - (x_2 - x_1)^2\right| R_1^2}{\left[(y_2 - y_1 + R_2)^2 + (x_2 - x_1)^2\right]^2} \tag{12}$$

$$m_{21} = \frac{2(y_2 - y_1 + R_2)(x_2 - x_1) R_1^2}{\left[(y_2 - y_1 + R_2)^2 + (x_2 - x_1)^2\right]^2} \tag{13}$$

$$n_{21} = -l_{21} \tag{14}$$

where R is the bubble radius and x_1 (x_2) and y_1 (y_2) are the x and y positions of the center of bubble 1(2). Later, it has been shown[8] that tailing bubbles have no significant influence on the leading bubbles. The simplified model reported in Ref. 8 was used in this work to modify the bubble velocity induced by neighbor bubbles as follows:

$$v_{y,2} = \begin{cases} v_{b\infty,2} + l_{21} v_{b\infty,1} & , \ (y_d - R_2)^2 + x_d^2 > R_1^2 \\ v_{b\infty,2} + v_{b\infty,1} & , \ (y_d - R_2)^2 + x_d^2 \le R_1^2 \end{cases} \tag{15}$$

$$v_{x,2} = \begin{cases} m_{21} v_{b\infty,1} & , \ (y_d - R_2)^2 + x_d^2 > R_1^2 \\ 0 & , \ (y_d - R_2)^2 + x_d^2 \le R_1^2 \end{cases} \tag{16}$$

where x_d and y_d the center-to-center distances between two bubbles in the x and y directions, respectively.

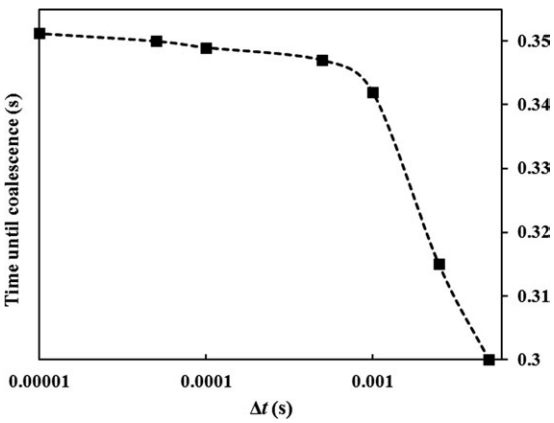

Figure 8. Dependency of predicted results on the time step.

Table 2. Simulation Conditions

Time step, Δt (s)	0.0001
Grid size, Δx and Δy (m)	0.01
Initial bed height, H_0 (m)	0.15, 0.3, 0.45
Bed width, W (m)	0.3
Bed thickness, δ (m)	0.015
Emulsion phase density, ρ_e (kg/m^3)	1300
Gas phase density, ρ_g (kg/m^3)	1.5
Minimum fluidization velocity, u_{mf} (m/s)	0.18
$(u_0 - u_{mf})/u_{mf}$	0.5–2.5

In a freely bubbling fluidized bed, the effect of all neighbor bubbles has to be taken into account. In other words, the modification term accounting for the effect of wake of leading bubbles exerted on bubble (i) can be expressed as

$$v_{y,i} = \begin{cases} v_{b\infty,i} + \sum_{j \ne i}^{nb} l_{ij} v_{b\infty,j} & , \ (y_d - R_i)^2 + x_d^2 > R_j^2 \\ v_{b\infty,i} + v_{b\infty,j} & , \ (y_d - R_i)^2 + x_d^2 \le R_j^2 \end{cases} \tag{17}$$

$$v_{x,i} = \begin{cases} \sum_{j \ne i}^{nb} m_{ij} v_{b\infty,j} & , \ (y_d - R_i)^2 + x_d^2 > R_j^2 \\ 0 & , \ (y_d - R_i)^2 + x_d^2 \le R_j^2 \end{cases} \tag{18}$$

The summation is performed for the bubbles contained in the neighbor list (nb) of bubble (i). Note that in this model, the interaction between a pair of bubbles is not a two-way interaction, because it was assumed that the tailing bubble has not any considerable effect on the velocity of leading bubble. The bubble interaction formula shows that the effect of bubbles at relatively remote locations relative to bubble (i) is not significant. To save computation time, a neighbor list shown in Figure 2 was considered. For each bubble, as

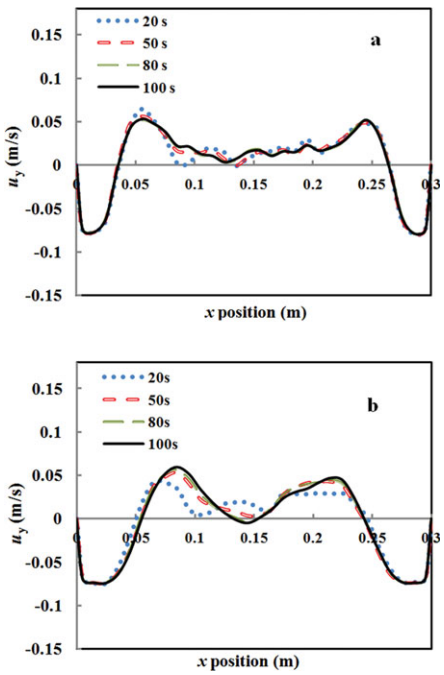

Figure 9. Lateral profiles of the emulsion phase vertical velocity: effect of time-averaging period, [(u_0 − u_{mf})/u_{mf} = 1.5]; (a) h = 0.1 m and; (b) h = 0.3 m above the distributor plate.

[Color figure can be viewed in the online issue, which is available at wileyonlinelibrary.com.]

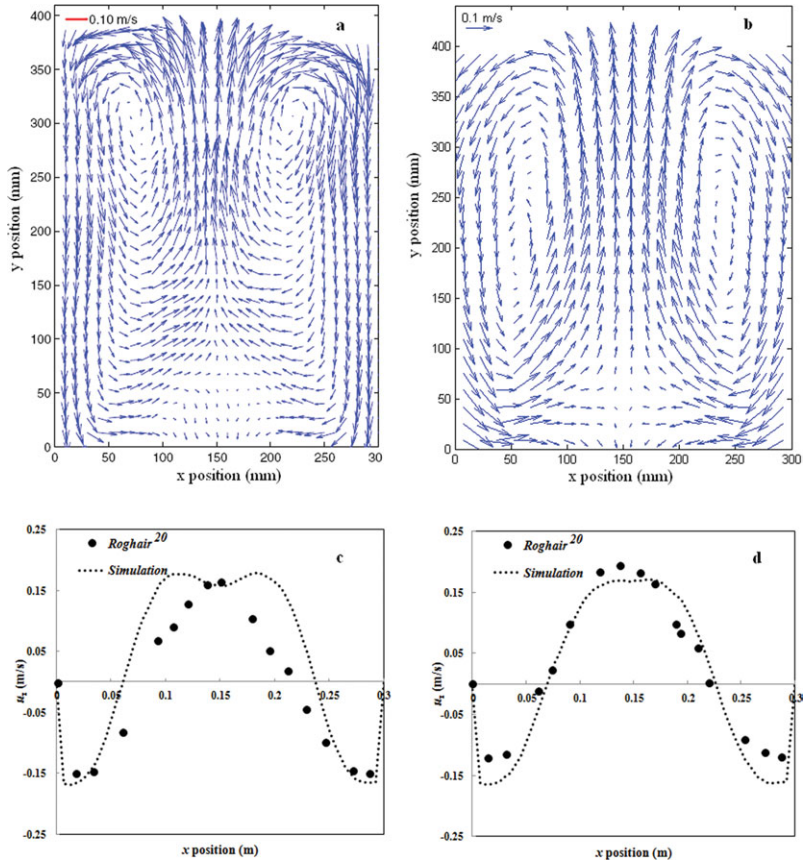

Figure 10. (a) Time-averaged emulsion phase velocity vector field experimentally determined by Laverman et al.[18] and (b) the vector field predicted by the present model. (c,d) lateral profile of the time-averaged emulsion phase velocity compared with the experimental data reported by Roghair[20], at $(u_0 - u_{mf})/u_{mf} = 2.5$.

[Color figure can be viewed in the online issue, which is available at wileyonlinelibrary.com.]

shown in this figure, the gray bubbles are in the neighbor list of the black bubble. Figure 3 shows the variations of l_{ij} with the dimensionless bubble distance factor (i.e., the distance between two bubbles divided by d_i) for two bubbles positioned according to this figure. This figure shows that the coefficient l_{ij} converges to zero for the dimensionless distances larger than five. Thus, in this work, L_2 (Figure 2) was taken as the fivefold bubble diameter.

In freely bubbling fluidized beds, gas can flow through bubble boundaries. This phenomenon plays a key role in accelerating the rear bubble upward. In this DBM, the volume change of bubbles because of gas leakage was not considered in the course of interaction. In fact, in this model, the modification term of the bubble–bubble interactions is responsible for the acceleration of bubbles because the bubble diameter was assumed to be constant as supposed by Clift and Grace.[8,9]

Coalescence

Coalescence of bubbles in fluidized beds is considered as one of the main reasons for bubble growth. In a number of previous DBM works, the coalescence phenomenon has been treated as a sudden phenomenon whenever two bubbles touch each other, but in fact, it is not a sudden phenomenon.[9] In this work, bubbles were treated as individual circular disks, but in real beds the gas bubbles usually have a spherical cap shape with a wake that its angle (θ_w) is not 180° as shown in Figure 1. A coalescence scenario, which is more realistic than sudden coalescence, is shown in Figure 4. In this scenario, the coalescence can take place when the nose of a tailing bubble reaches the line AA' of the leading bubble. A constant wake angle of 120° was considered for the bubbles based on the size of particles and the experimental findings of Rowe and Partridge.[15] Figure 4 shows the coalescence criteria for a pair of bubble schematically. When bubbles move up in the bed, the tailing bubble tends to move behind the leading bubble (I→II). Then, the nose of tailing bubble enters the wake region of the leading bubble (i.e., dashed region in the bubble presented in Figure 1) just under the line AA' (III), therefore, in this scenario, the overlap of bubbles is allowed. Once the tailing bubble passes through the line AA', the two bubbles coalesce and form a new larger bubble (IV).

Note that the force balance equations which were derived for circular shape bubbles are valid until the nose of a tailing bubble enters the bottom of the leading bubble. After that, the tailing bubble's velocity could be determined by Eqs. 15–16 (i.e., $v_{y,i} = v_{b\infty,i} + v_{b\infty,j}$ and $v_{x,i} = 0$). The information of wake angle were used to postpone the coalescence of bubbles only.

Emulsion phase velocity

Mori et al.[16] proposed a model for steady-state radial distribution of bubbles in a 2-D bed. Later, Kobayashi et al.[17] developed a numerical model, which could estimate the bubble distribution and circulation pattern of solids in

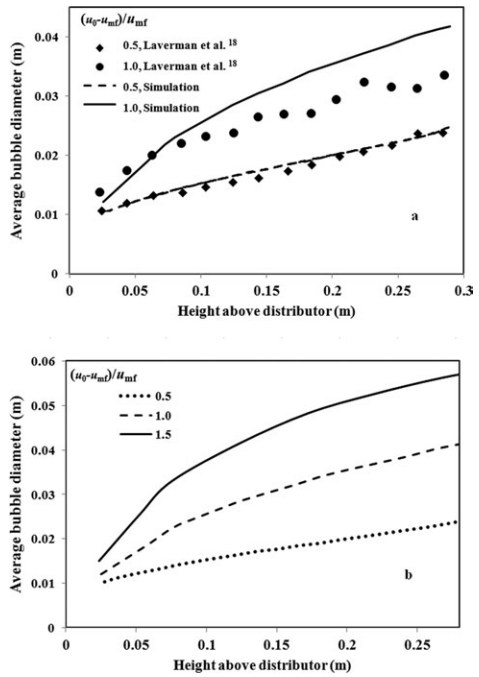

Figure 11. (a) Average bubble diameter vs. height above the distributor compared with experimental data reported by Laverman et al.,[18] and (b) simulation results for average bubble diameter vs. height above distributor at different superficial gas velocities.

bubbling fluidized beds on the basis of the model developed by Mori et al. Their model was not a dynamic model, but it could predict the stationary solid flow patterns. The predicted radial distribution of particle vertical velocity by Kobayashi et al.[17] shows a downward solid motion near the walls and an upward motion near the center of the bed.

As mentioned earlier, the modification term in the equations of the bubble–bubble interaction presented by Clift and Grace[9] is the emulsion phase velocity at the nose of bubble if the bubble is absent. On the basis of potential flow assumptions around a single bubble, the dense phase velocity may be evaluated by the equations of bubble–bubble interactions using a second bubble with zero radius on all of the grid points. Note that the assumption of zero radius for a bubble leads to a zero value for the bubble rise velocity in isolation ($v_{b\infty}$) in Eq. 11-a, hence, the emulsion phase velocity remains in right-hand side (RHS) of the equation only. The flow pattern around a single bubble is the same as Davidson bubble (Figure 5a). In this work, for swarm of bubbles, the superposition rule was used to determine the velocity vector field around the bubbles. The basis of this assumption is the fact that (at least for Geldart B type particles) the emulsion phase velocity induced by the bubbles is much larger than that induced by the interstitial gas. Thus, the equation of emulsion phase velocity for a grid point (i,j) can be written as

$$u_y(i,j) = \sum_k^{nb} \left(l_{(i,j)k} v_{y,k} + m_{(i,j)k} v_{x,k}\right) \tag{22}$$

$$u_x(i,j) = \sum_k^{nb} \left(m_{(i,j)k} v_{y,k} + n_{(i,j)k} v_{x,k}\right) \tag{23}$$

where $l_{(i,j)k}$,$m_{(i,j)k}$, and$n_{(i,j)k}$ are given by

$$l_{(i,j)k} = \frac{\left[\left(y_{(i,j)} - y_k\right)^2 - \left(x_{(i,j)} - x_k\right)^2\right] R_k^2}{\left[\left(y_{(i,j)} - y_k\right)^2 + \left(x_{(i,j)} - x_k\right)^2\right]^2} \tag{24}$$

$$m_{(i,j)k} = \frac{2\left(y_{(i,j)} - y_k\right)\left(x_{(i,j)} - x_k\right) R_k^2}{\left[\left(y_{(i,j)} - y_k\right)^2 + \left(x_{(i,j)} - x_k\right)^2\right]^2} \tag{25}$$

$$n_{(i,j)k} = -l_{(i,j)k} \tag{26}$$

Moreover, the summation is performed over a neighbor list (*nb*) of bubbles near the reference point. The neighbor list of the point (i,j) is schematically depicted in the bottom part of Figure 2 by the dashed bubbles. The neighbor list is the list of bubbles shown in a square with length L_1. In this work, L_1 was chosen 10-fold the maximum bubble size existing in the bed to be sure that the effects of all near bubbles were considered for the velocity calculation. The induced flow pattern of emulsion phase due to the rise of a single bubble as well as swarm of bubbles is shown in Figure 5.

Solution method

A time driven approach was used for the bubble tracking. Figure 6 shows a flowchart of the solution algorithm. For each time step, the Newtonian's equation of motion for each bubble (i.e., Eq. 1) was integrated to determine the new position of bubble. For bubble removal from the bed surface, the gas bubbles, which their bottoms crossed the bed surface were removed from the bubble list. In addition, on the basis of the precalculated bubble injection frequency; bubbles with uniform sizes were injected from the region below the distributor plate. In this model, the emulsion phase affects the motion of a bubble when the bubble's bottom reaches the distributor baseline. The vector field of the emulsion phase was determined by the method described in the previous section after repositioning of the bubbles. Then, the new bubble velocities were calculated using the bubble force balance (i.e., Eq. 1). The new velocity of bubble was subsequently modified to account for the effect of wake forces. At the next stage, an overlap checking routine detected possible overlap of bubbles. The overlap of more than two bubbles was permitted but the bubble at the highest position in a bubble cluster (overlapped bubbles) was supposed to be the

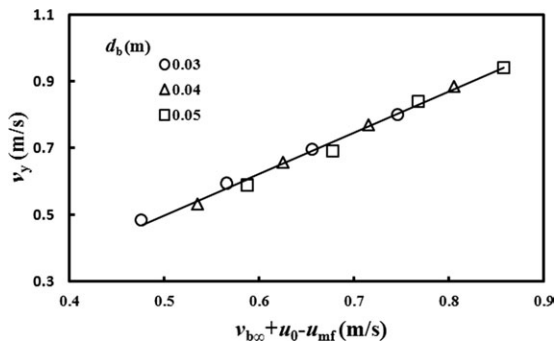

Figure 12. Variations of the vertical velocity of the bubbles with $v_{b\infty} + (u_0 - u_{mf})$ for three different bubble diameters.

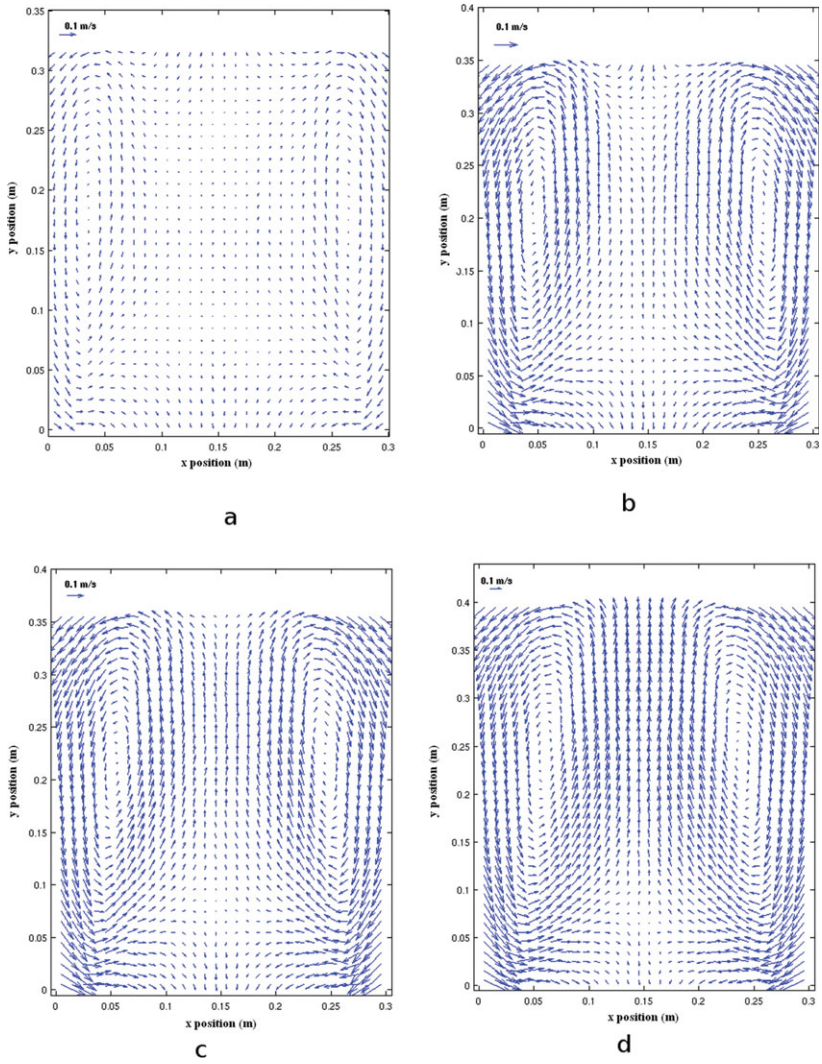

Figure 13. Time-averaged emulsion phase velocity profiles at (a) $(u_0 - u_{mf})/u_{mf} = 0.5$, (b) $(u_0 - u_{mf})/u_{mf} = 1.0$, (c) $(u_0 - u_{mf})/u_{mf} = 1.5$, and (d) $(u_0 - u_{mf})/u_{mf} = 2.0$.

[Color figure can be viewed in the online issue, which is available at wileyonlinelibrary.com.]

leading bubble. For clusters with more than two overlapping bubbles, an ascending sort was performed based on the axial position of the bubbles in the bed and, coalescence criteria were only checked for the first couple. Possible collisions with the walls were also checked for each bubble and, the velocity of bubbles colliding with walls changes with the assumption of elastic (i.e., mass and momentum conservative) collisions. The ideal collisions are an approximation of reality, since it is simply unknown how bubbles behave once they get close to the wall. These steps were repeated until the total time of simulation reaches T_{stop}.

Dependency of the solution on the grid size and time step

To examine the mesh dependency of the developed model, a bed with the dimensions of 0.16×0.16 m^2 was simulated under the conditions of different cell sizes and, the predicted results are shown in Figure 7. This figure shows the variations of the vertical velocity of emulsion phase at a height of 0.3 m above the distributor with the bed width for different cell sizes. It can be seen from this figure that for cell sizes less than $\Delta x = \Delta y = 0.01$ m, the averaged profiles are almost the same. Furthermore, a simple test was conducted to show the reliable time step in the simulations. In this regard, two bubbles were injected in the bed with a delay time of 0.02 s while bubbles were not in vertical alignment. The time needed to these two bubbles coalesce and make a larger bubble vs. the time step (Δt) is shown in Figure 8. This figure shows that for the time steps less than 0.0001 s, the simulations results are almost the same. Thus, in the simulations, $\Delta t = 0.0001$ s was chosen as the time step to guarantee the independency of the results on the time step.

Simulation conditions

Experimental data reported by Laverman et al.,[18] Laverman,[19] and Roghair[20] were used to validate the simulation results. They used 400−600 μm spherical glass particles in a pseudo-2-D fluidized bed. In this work, a 0.3 m wide pseudo-2-D bed with different initial bed heights and superficial gas velocities was, also, simulated. The initial bed height to width ratio was set to 0.5−1.5 to study the effect of different bed aspect ratios. The gas injection velocity ranges from 1.5 to 3.5 u_{mf}. To mimic a porous plate distributor, a random number generator was used to generate the bubble injection positions. Other conditions are summarized in Table 2.

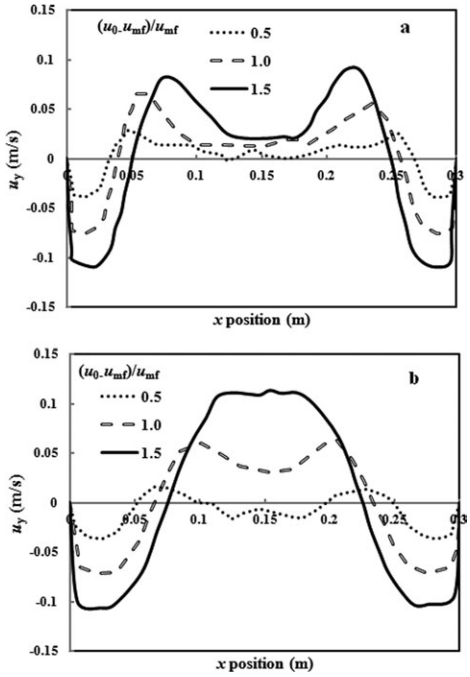

Figure 14. Lateral profiles of the time-averaged emulsion phase vertical velocity for different superficial gas velocities (a) at h = 0.1 m and (b) at h = 0.3 m above the distributor plate.

According to the two-phase theory, all gas in excess of the amount required to fluidize particles at minimum fluidization condition, passes through the bed as gas bubbles.[21] However, it was experimentally found that only a fraction of the excess gas (i.e., $u_0 - u_{mf}$) passes through the bed as gas bubbles. Werther[22] has measured the fraction of the excess gas that is observable as bubbles for particles belonging to different types of Geldart's particle classification. For particles of Geldart B type, which were used in this work, this fraction (relative visual bubble flow rate) is about 0.65. Using this data and specifying an initial bubble diameter, the bubble number frequency at the distributor could be calculated. In this work, bubbles with identical initial diameters were used, which vary from 0.80 to 1.5 cm for different superficial gas velocities (i.e., from 1.5 to 3.5 u_{mf}, respectively). Note that the values of these initial bubble diameters were chosen based on the extrapolation of the experimental data reported by Laverman et al.[19]

Model Validation

First, it is important to verify that time-averaging was performed over a sufficiently long time period. For this purpose, the results of simulation at $(u_0 - u_{mf})/u_{mf} = 1.0$ are shown in Figures 9a, b using different time periods for averaging. These figures show the averaged vertical component of the emulsion phase velocity at two different heights above the distributor. The time-averaged velocity profiles show that the simulation results do not change considerably after t = 80 s. Therefore, all simulation results were time-averaged over at least 80 s. The experimental data reported by Laverman et al.[18], Laverman,[19] and Roghair[20] were used to validate the model predictions. They used a PIV technique to determine the vector field of solid particles as well as DIA to determine the bubble characteristics such as bubble diameter and velocity distributions in a pseudo-2-D fluidized bed. They modified the PIV raw data using a hybrid DIA + PIV technique to account for the solid porosity profiles to obtain the solid mass flux profiles.[18–20]

Figures 10a, b show the experimental and simulated time-averaged vector field of the emulsion phase in a 0.30 m wide pseudo-2-D fluidized bed. It can be seen that, the developed model predicts the vortices present in the top half of the bed, the downward motion near the walls, and the upward motion in the middle part of the bed. Figures 10c, d show the vertical velocity profiles of emulsion phase at two different heights. It can be observed from these figures that the predicted results are in good agreement with the experimental data. In addition, the estimated radial distribution of particle vertical velocity by Kobayashi et al.[17] shows the same trend as the time-averaged results obtained in this work. In addition, Figure 11a shows the average bubble diameter vs. height above the distributor for two different superficial gas velocities. This figure clearly demonstrates that the predicted evolution of the bubble size is in fair agreement with the experimental data.

Results and Discussion

In this section, the effects of various important variables and parameters on the average bubble diameter and emulsion phase circulation pattern are presented and discussed.

Effect of superficial gas velocity

In this developed model, bubbles grow only due to the coalescence. In the Geldart B and D particle systems, the gas bubbles can grow without limit, whereas for fine particle systems, bubbles larger than a maximum size collapse from the roof.[22] Generally, the bubble diameter is expressed as the equivalent diameter of a spherical bubble in 3-D beds or a disk shape bubble in 2-D beds. Figure 11b shows the predicted values of average bubble diameter as a function of bed height above the distributor. Increasing the superficial gas velocity increases the initial bubble diameter and bubble injection frequency at the distributor, therefore, at larger gas velocities, the average bubble diameter is expected to be larger at the same height in the bed. Large bubbles drag particles with larger velocities in their wakes and, also, particles move aside around a bubble with higher velocities. For a single isolated bubble, based on the relation of Davies and Taylor,[11] the bubble velocity increases with the square root of the bubble diameter. Increasing the velocity of bubbles is

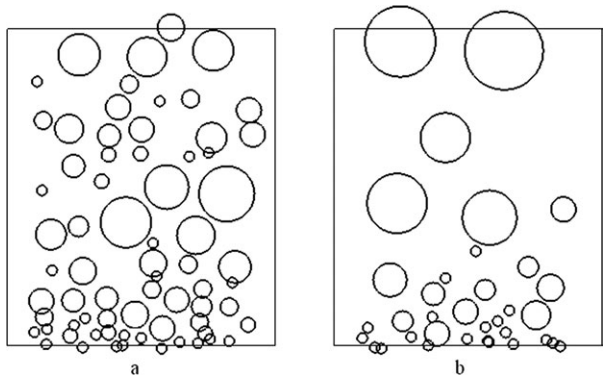

Figure 15. Snapshots of the bubbles present in the bed (a) without and (b) with taking into account bubble interactions, $(u_0 - u_{mf})/u_{mf}$ = 1.5.

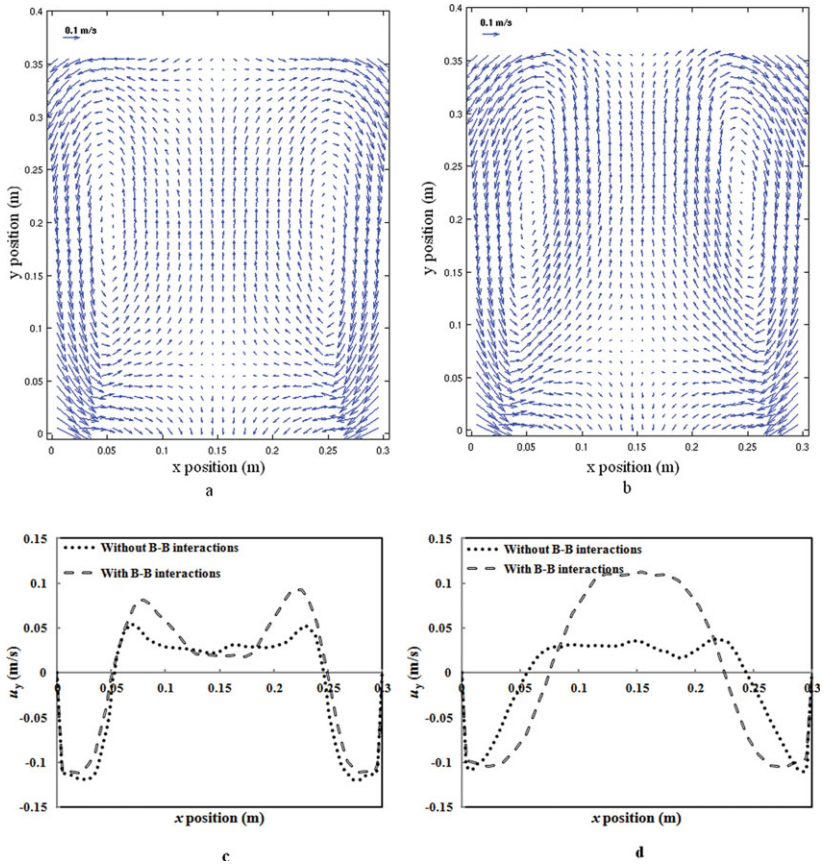

Figure 16. Time-averaged emulsion phase velocity profiles at $(u_0 - u_{mf})/u_{mf} = 1.5$ (a) without and (b) with taking into account bubble–bubble interactions; and the lateral profiles of the time-averaged emulsion phase vertical velocity at (c) $h = 0.10$ m and (d) $h = 0.30$ m above the distributor plate.

[Color figure can be viewed in the online issue, which is available at wileyonlinelibrary.com.]

more pronounced for bubbles moving in a swarm. Figure 12 shows the variation of the averaged-vertical velocity of the bubbles in the bed for three different diameters with $v_{b\infty} + (u_0 - u_{mf})$. It can be seen from this figure that almost all the predicted data lie on the same line. This figure shows that the bubble rising velocity increases with an increase in the excess gas velocity with a constant slope. Note that presented correlations for the bubble rise velocity in freely bubbling beds often contain the spurious term $(u_0 - u_{mf})$ added to the velocity. This has no physical meaning, and speculation has been that the bubble interaction is what causes the rise velocity to be higher than that of a single bubble. The discussions in this article are consistent with this.

Figures 13a–d show the vector fields of time-averaged emulsion phase velocity for different superficial gas velocities. Figures 14a, b show the vertical velocity of the

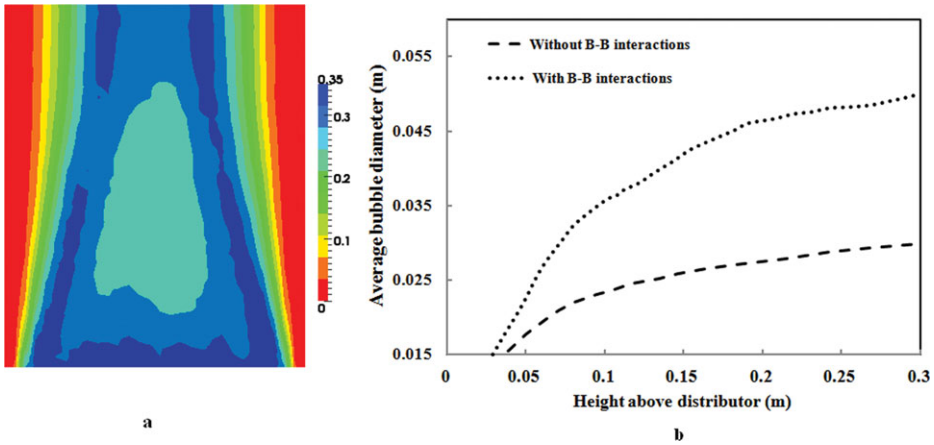

Figure 17. (a) Averaged bubble induced void fraction in the bed with the effect of bubble–bubble interactions, and (b) Average bubble diameter with and without accounting for bubble–bubble interactions $[(u_0 - u_{mf})/u_{mf} = 1.5]$.

[Color figure can be viewed in the online issue, which is available at wileyonlinelibrary.com.]

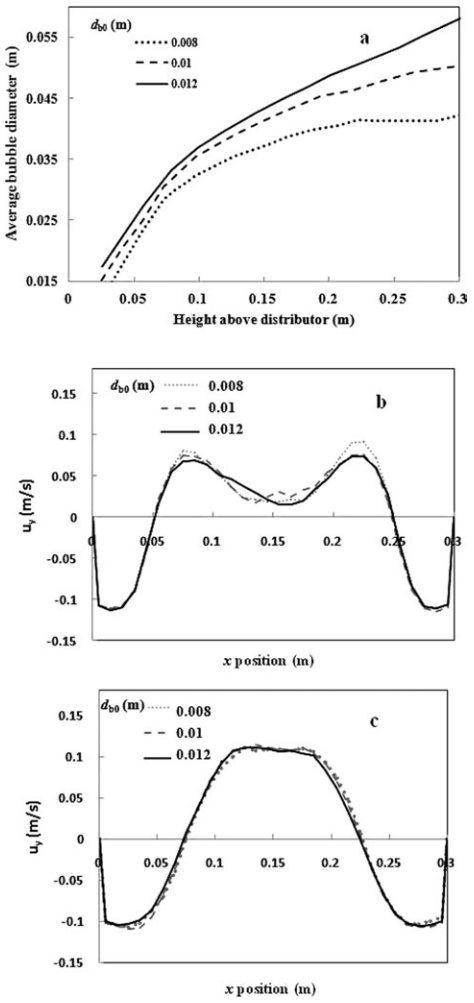

Figure 18. (a) Averaged bubble diameter vs. height above the distributor for different initial bubble diameter at a constant superficial gas velocity [$(u_0 - u_{mf})/u_{mf} = 1.5$], and the lateral profiles of the time-averaged emulsion phase vertical velocity at (b) $h = 0.10$ m and (c) $h = 0.30$ m above the distributor plate for different initial bubble diameter [$(u_0 - u_{mf})/u_{mf} = 1.5$].

emulsion phase at two different heights and different superficial gas velocities. Increasing the superficial gas velocity causes the profiles of the emulsion phase velocity to become more pronounced, that is, larger upward and downward velocities and solid circulation. The average upward velocity of particles at a height of 0.3 m is about two times greater than that of at height of 0.1 m for $(u_0 - u_{mf})/u_{mf} = 1.5$. Moreover, this value at $(u_0 - u_{mf})/u_{mf} = 1.5$ is about sixfold average upward velocity at $(u_0 - u_{mf})/u_{mf} = 0.5$.

Effect of bubble−bubble interactions

As mentioned earlier, bubble–bubble interactions have a profound effect on the profile of the emulsion phase velocity and bubble behavior in the bed. Krishna and van Baten[7] have reported that the bubble velocity increases by a factor of 1.5–3.0 due to the effect of interactions. Bubble–bubble interaction enforces bubbles located at the bottom part of the bed to move toward the centerline of the bed because of the effect of the wake force of leading bubbles in the bed. Figure 15 shows snapshots of the bed for two different cases: a bed with bubble–bubble interactions accounted for (right) and a bed neglecting these interactions (left). Figures 16a–d demonstrate the vector field of time-averaged emulsion phase velocity and the lateral profile of the emulsion phase velocity at two different heights of the bed compared with those predicted without accounting for bubble–bubble interactions. As may be observed from Figure 16d, at the top of the bed, the vertical velocity of the emulsion phase increases considerably due to the effect of bubble–bubble interactions at $(u_0 - u_{mf})/u_{mf} = 1.5$. It can be seen from Figure 16d that the average particle upward velocity decreases about three times with ignoring bubble–bubble interactions. Figure 17a shows the bubble induced void fraction of the bed averaged over 100 s, taking bubble–bubble interactions into account in the model. This figure also shows the average bubble path in the bed. Figure 17b shows variations of average bubble diameter with the height above the distributor for two cases (i.e., with and without interactions). This figure clearly shows that bubble–bubble interactions are quite important for predicting the average bubble size accurately.

Effect of initial bubble diameter

In DBM, the initial bubble diameter is fixed by the user. In this work, an identical initial bubble diameter (without any bubble size distribution) was used. Increasing the bubble diameter at a constant superficial gas velocity decreases the bubble frequency. Figure 18a shows the average bubble diameter evolution at $(u_0 - u_{mf})/u_{mf} = 1.5$ with different initial bubble diameters. This figure demonstrates that in the regions near the distributor, the different initial bubble diameters did not show profound obvious influences on the bubble growth behavior, but at the higher regions, the results of the cases with greater initial diameters have larger average bubble diameters. Moreover, Figures 18b, c demonstrate the average vertical velocity profiles of the emulsion phase at two different heights above the distributor. These figures clearly show that the initial bubble diameter do not show significant influences on the profiles of the emulsion phase velocity. Note that this behavior has been also reported by the Bokkers et al.[3]

Effect of the bed aspect ratio

The effect of the bed aspect ratio on the emulsion phase behavior was also studied. Figures 19a, b show the time-averaged emulsion phase flow patterns at $(u_0 - u_{mf})/u_{mf} = 1.5$ for two different initial bed heights. Figures 19c, d also show the development of the lateral profiles of the vertical emulsion phase velocity as a function of the bed height. In the simulation, the superficial gas velocity was varied from 1.5 to 3.5 u_{mf}. In this range of superficial gas velocity, all the profiles show the same trend. A double peak upward velocity profile can be seen near the distributor. This behavior can be explained by the bubble movements toward the centerline of the bed. At the higher positions, the gas bubbles tend to move to the center of the bed mainly because of the effects of bubble–bubble interactions and coalescence and, hence, the double peak profile changes to a single peak with larger velocity magnitude. It is clear that the variation of the bed aspect ratio does not vary the path of the bubbles significantly. Moreover, for low bed aspect ratios, gas bubbles erupt at the surface before arriving at the bed center and, hence, the

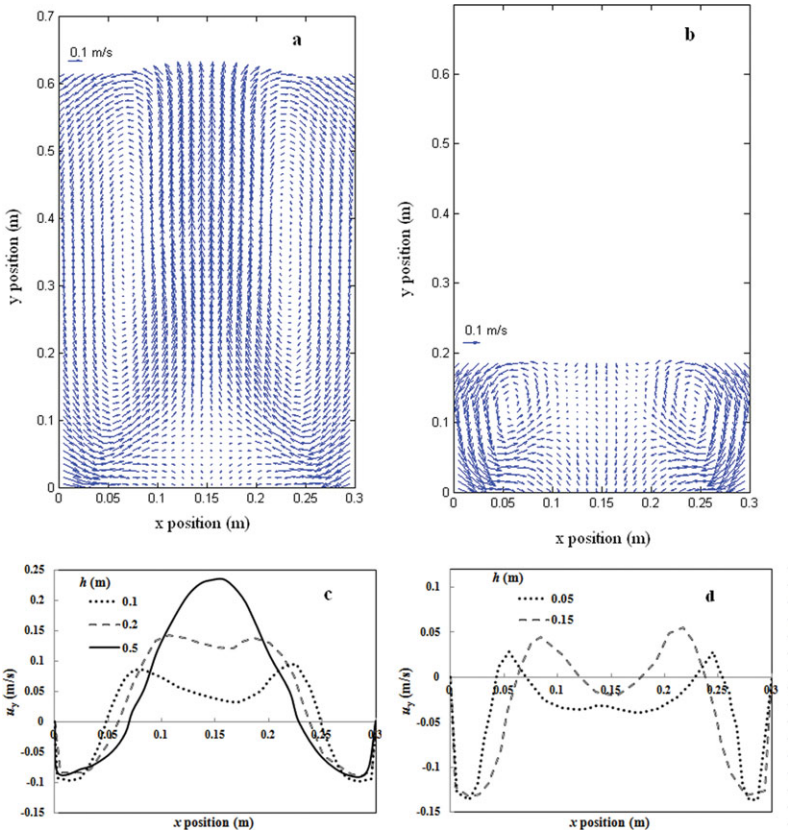

Figure 19. Time-averaged emulsion phase velocity profiles at $(u_0 - u_{mf})/u_{mf} = 1.5$ (a) initial bed height of 0.45 m (b) initial bed height of 0.15 m, and the lateral profiles of the time-averaged emulsion phase vertical velocity at different heights for (c) bed with $H_0 = 0.45$ m and (d) bed with $H_0 = 0.15$ m.

[Color figure can be viewed in the online issue, which is available at wileyonlinelibrary.com.]

vertical velocity profile near the bed surface (i.e., $h = 0.15$ m) remains a double peak (Figure 19d).

Figure 19d also shows that the developed model does not guarantee continuity of the emulsion phase (i.e., up flow = down flow over a horizontal cross section). The main reason for this fact is that the equation of mass balance for solid phase did not play any role in the developed model, therefore, it is better to modify this model by coupling it with equation of mass balance in the future works.

Conclusions

A PDBM has been developed and tested successfully for 2-D gas–solid freely bubbling fluidized beds. The developed model can be efficiently applied for pseudo-2-D beds. It was found that:

- The developed model can predict the time-averaged emulsion phase velocity profiles and the bubble diameter evolution as a function of height above the distributor satisfactorily. The predicted results are in fair agreement with reported experimental data.
- At larger superficial gas velocities and at the same height, the time-averaged vertical emulsion phase velocity profiles are more pronounced than those predicted at low superficial gas velocities.
- Averaged-macroscopic emulsion phase circulation patterns clearly show upward motion in the central part of the bed and a downward motion near the walls. At heights near the distributor, these profiles show a double peak, whereas at higher levels, the profiles change to single peak with larger up-flow values.
- Bubble–bubble interactions influence the behavior of emulsion and bubble phases drastically. Moreover, snapshots of the bed and the results of averaged-bubble diameter show that the coalescence frequency increases by introducing this effect into the model. The profiles of averaged-bubble induced void fraction in the bed show that bubbles have a tendency to move to the center of the bed when they travel upward because of this effect.
- Changing the initial bubble diameter at a constant superficial gas velocity varies bubble growth behavior but the emulsion phase behavior remains almost the same.
- Study of beds with different bed aspect ratios shows that changing the initial bed height does not vary the bubble movement considerably. In beds with $\frac{H_0}{W} \leq 1$, the mentioned double peak in the emulsion up-flow profiles could not develop to the single peak profiles even near the bed surface. This is because of the fact that the bubbles leave the bed before coalescence with the bubbles located in the center of the bed.
- One of the weaknesses of the present model is that the model does not guarantee the continuity of the emulsion phase (i.e., up flow = down flow over a horizontal cross section). The main reason for this fact is that the equation of mass balance for solid phase did not play any role in the developed model, therefore, it is better to modify this model by coupling it with the equation of mass balance in the future works.

Notation

c = constant in single bubble rising velocity
C_D = drag coefficient
C_{vm} = virtual mass coefficient
d_b = bubble diameter, m
d_e = equivalent bubble diameter, m
$\vec{F}_D$ = drag force, N
$\vec{F}_G$ = gravity force, N
$\vec{F}_p$ = pressure force, N
$\vec{F}_t$ = total forces acting on a bubble, N
$\vec{F}_{VM}$ = virtual mass force, N
$\vec{g}$ = gravity acceleration, m/s^2
h = height above the distributor, m
H_0 = initial particle height in the bed, m
L_1 = length of neighbor list box for the calculation of emulsion velocity, m
L_2 = edge of neighbor list box for the calculation of bubble–bubble interactions, m
l_{ij} = coefficient for bubble velocity modification
m_{ij} = coefficient for bubble velocity modification
m_b = bubble mass, kg
n_{ij} = coefficient for bubble velocity modification
nb = neighbor list
R = bubble radius, m
t = time, s
T_{stop} = total simulation time, s
u_0 = superficial gas velocity, m/s
$\vec{u}$ = emulsion phase velocity, m/s
u_{mf} = minimum fluidization velocity, m/s
$\vec{v}$ = bubble velocity, m/s
v_{br} = bubble rise velocity, m/s
$v_{b\infty,i}$ = bubble rise velocity in isolation, m/s
$v_{x,i}$ = x component of the velocity of bubble (i), m/s
$v_{y,i}$ = y component of the velocity of bubble (i), m/s
V_b = bubble volume, m^3
W = bed width, m
x = x position, m
y = y position, m
x_d = distance between two bubble in x-direction, m
y_d = distance between two bubble in y-direction, m
P = pressure, Pa

Subscripts and superscripts

i = bubble number and grid indicator in x-direction
j = bubble number and grid indicator in y-direction

Greek letters

ρ_g = gas density, kg/m^3
ρ_e = emulsion bulk density, kg/m^3
δ = pseudo-2-D bed thickness, m
θ_w = wake angle of bubble, °

Acknowledgments

The first two authors are grateful for financial support provided by ministry of science, research, and technology of Iran.

Literature Cited

1. Delnoij E, Lammers FA, Kuipers JAM, van Swaaij WPM. Dynamic simulation of dispersed gas–liquid two-phase flow using a discrete bubble model. *Chem Eng Sci*. 1997;52:1429–1458.
2. Darmana D, Deen NG, Kuipers JAM. Detailed modeling of the hydrodynamics mass transfer and chemical reactions in a bubble column using a discrete bubble model. *Chem Eng Sci*. 2005;60:3383–3404.
3. Bokkers GA, Laverman JA, van Sint Annaland M, Kuipers JAM. Modelling of large sclae dense gas-solid bubbling fluidised beds using a novel discrete bubble model. *Chem Eng Sci*. 2006;61:5590–5602.
4. Laverman JA, van Sint Annaland M, Kuipers JAM. *Investigation of the Influence of Bubble–Bubble Interaction on the Hydrodynamics of Bubbling Gas-Solid Fluidized Beds Using the Discrete Bubble Model*, Fifth International Conference on CFD in the Process Industries, CSIRO, Melbourne, Australia, 2006.
5. Pannala S, Daw CS, Halow JS. Simulations of reacting fluidized beds using an agent-based bubble model. *Int J Chem React Eng*. 2003;1:1–18.
6. Pannala S, Daw CS, Halow JS. Dynamic interacting bubble simulation (DIBS): an agent-based bubble model for reacting fluidized beds. *Chaos*. 2004;14:487–498.
7. Krishna R, van Baten JM. Using CFD for scaling up gas–solid bubbling fluidised bed reactors with Geldart A powders. *Chem Eng J*. 2001;82:247–257.
8. Clift R, Grace JR. *Continuous Bubbling and Slugging in: Fluidization*, 2nd ed. London: Academic Press, 1985.
9. Clift R, Grace JR. Coalescence of bubbles in fluidized beds. *AIChE Symp Ser*. 1971;67:23–33.
10. De Korte RJ, Schouten JC, van den Bleek CM. Controlling bubble coalescence in a fluidized-bed model using bubble injection. *AIChE*. 2001;47:851–860.
11. Davies RM, Taylor GI. The mechanics of large bubbles rising through extended liquids and through liquids in tubes. *Proc R Soc London*. 1950;200:375–390.
12. Mudde RF, Schulte HBM, van den Akker HEA. Analysis of a bubbling 2-d gas-fluidized bed using image processing. *Powder Technol*. 1994;81:149–159.
13. Shen L, Johnsson F, Leckner B. Digital image analysis of hydrodynamics two-dimensional bubbling fluidized beds. *Chem Eng Sci*. 2004;59:2607–2617.
14. Auton TR. *The Dynamics of Bubbles, Drops and Particles in Motion in Liquids*. PhD Thesis, Cambridge University, 1983.
15. Rowe PN, Partridge BA. An X-ray study of bubbles in fluidised beds. *Trans Inst Chem Eng*. 1965;43:157–175.
16. Mori S, Miho S, Yamada M, Hiraoka S, Yamada I. Radial distribution of bubbles in the cylindrical fluidized bed. *AIChE Symp Ser*. 1984;241:10–16.
17. Kobayashi N, Yamazaki R, Mori S. A study on the behavior of bubbles and solids in bubbling fluidized beds. *Powder Technol*. 2000;113:327–344.
18. Laverman JA, Roghair I, van Sint Annaland M, Kuipers H. Investigation into the hydrodynamics of gas–solid fluidized beds using particle image velocimetry coupled with digital image analysis. *Can J Chem Eng*. 2008;86:523–535.
19. Laverman JA. On the hydrodynamics in gas phase polymerization reactors. PhD Thesis, Eindhoven University of Technology, Eindhoven, 2010.
20. Roghair I. *Development of an Experimental Method to Investigate the Hydrodynamics in a Fluidized Bed using PIV and DIA*. Master Thesis, Twente University, 2007.
21. Toomey RD, Johnstone HF. Gaseous fluidization of solid particles. *Chem Eng Prog*. 1952;48:220–226.
22. Werther J. *Fluidized-bed reactors*. In: Elvers, BHawkins, SSchulz, G. editors. *Principles of Chemical Reaction Engineering and Plant Design, Vol. B4 of Ullmann's Encyclopedia of Industrial Chemistry*, fifth ed. VCH Verlagsgesellschaft mbH, Weinheim, 1992.

Manuscript received July 6, 2011 and revision received Nov. 14, 2011.